J Mater Sci (2009) 44:6795–6804
DOI 10.1007/s10853-009-3682-6

MESOSTRUCTURED MATERIALS

Cu(II) complexes imobilized on functionalized mesoporous silica as catalysts for biomimetic oxidations

M. Mureşeanu · V. Pârvulescu · R. Ene · N. Cioateră · T. D. Pasatoiu · M. Andruh

Received: 30 November 2008 / Accepted: 12 June 2009 / Published online: 23 June 2009

Abstract Mesoporous HMS silica was synthesized and functionalized with 3-aminopropyl-triethoxysilane (APTES) by a post-synthesis method. HMS and NH_2-HMS supports were used for immobilization of two Cu(II) biomimetic complexes ([Cu(acac)(phen)(H_2O)](ClO_4), [Cu(acac)(Me_2bipy)](ClO_4)) or laccase enzyme. Mesoporous structure of the support; functionalization of silica surface, structure of ligands, and Cu complexes; and their immobilization were evidenced by XRD analysis, N_2 adsorption–desorption, SEM microscopy, TGA-DTA, IR and UV–Vis spectroscopy, and elemental analysis. The results confirm the structural integrity of the mesoporous hosts and successful anchoring of the metal complexes over the supports. For comparison, copper-substituted mesoporous silica (Cu-HMS) by using dodecylamine as structure-directing agent was also synthesized. All the synthesized materials were tested for their catalytic activity on the oxidation of 4-aminoantipyridine, 2,2′-azinobis (3-ethyl-benzothiazoline)-sulfonic acid (ABTS) with air, as well as in liquid phase oxidation of anisole and phenol with hydrogen peroxide. In order to verify the complex biomimetic activity, the *Trametes versicolor* laccase was immobilized by adsorption in the same supports.

M. Mureşeanu (✉) · N. Cioateră
University of Craiova, Calea Bucuresti 107I, Craiova, Romania
e-mail: mihaela_mure@yahoo.com

V. Pârvulescu · R. Ene
Institute of Physical Chemistry, Splaiul Independetei 202, 060021 Bucharest, Romania

T. D. Pasatoiu · M. Andruh
Inorganic Chemistry Laboratory, Faculty of Chemistry, University of Bucharest, Str. Dumbrava Rosie no 23, 70254 Bucharest, Romania

Introduction

Porous nanostructured organic–inorganic hybrid materials have attracted considerable attention due to their specific applications [1]. The synthesis of new porous materials with controlled morphology and accessible metallic centers for the reactant molecules in their channels is still an important challenge for the design of new types of molecular sieves-like catalysts [2]. The interest for supramolecular metallic architectures containing copper is also illustrated by the literature, which indicates structures resulted from both Cu(II) and Cu (I) [2, 3]. A number of mono- and binuclear Cu(II) complexes have been investigated as biomimetic catalysts for catechol oxidation [4–6]. Copper (II) complexes have various applications in modern chemistry. They are used as catalysts in oxidation of cyclic, aliphatic, or aromatic compounds [7–9]; in enantioselective reactions [10]; or as biomimetic species [11].

The use of inorganic support materials with chemically bound active centers as heterogenized catalysts endows the homogeneous systems with attractive features such as easy product separation and catalyst stability and recovery. A range of synthetic procedures to attach organic moieties to the support surface are currently developed. The fixation of active biomimetic ligands via covalent bounding to a silica surface in order to be used in catalytic processes represents a remarkable aspect of the catalyst heterogenization. The functionalized alkoxysilanes such as 3-aminopropyl-triethoxysilane allow the subsequent bounding of the catalytic active species. This method was used for the immobilization of the synthetic structural mimics of the active centers of metalloenzymes on various supports, allowing obtaining artificial enzymes working efficiently [12, 13].

In the last decade a growing interest in the heterogenization of homogeneous metal complexes using several types of supports and several immobilization strategies has witnessed [14–17]. Initially, the complexes were just ion-exchanged or adsorbed on the porous supports and, consequently, could be susceptible to leaching [18, 19]. More recently, several grafting and tethering procedures have been developed to covalently attach transition-metal complexes to organic polymers [19], silica, zeolites, and other micro- and mesoporous inorganic materials [16–18]. The heterogeneous catalysts present similar catalytic parameters with those obtained in homogeneous-phase reaction under similar experimental conditions, and no significant metal complex leaching was observed after the catalytic reactions [20, 21]. The immobilization on several porous supports of (Schiff base) copper (II) complexes previously synthesized [22] or prepared in situ on the porous structure [23, 24] was reported. In addition, different substrates oxidation activity of laccase immobilized on nanoparticles and kaolinite [25] and some silica-supported copper (II) complexes [26] were also investigated.

The silica-based inorganic mesoporous materials which offer pore sizes in the range 20–100 Å are more suitable for liquid-phase reactions, because they allow easy diffusion of reactants to the active sites [25]. Their surface silanol groups can also be easily functionalized by using trialkyloxysilanes, with amine, thiol, carboxylic acid, phenyl, cyano, sulfonic acid, and vinyl groups, hence allowing subsequent chemical attachment of the catalytic active species, namely inorganic coordination compounds. Furthermore, they can be easily characterized by several spectroscopic techniques. Despite the hexagonal mesoporous silica (HMS) being less ordered than the MCM-41 and SBA-15 materials, they are much easier and straightforward to synthesize due to the use of a cheap and neutral template, i.e., long chain amines, which does not require strongly acidic conditions [27, 28]. The MCM class of materials has hexagonal long range order, while the HMS materials are considerably less ordered and are better described as *wormhole* structures [29].

The aim of this paper was synthesis and characterization of catalysts obtained by immobilization of Cu (II) biomimetic complexes ([Cu(acac)(phen) (H_2O)](ClO_4), [Cu(acac)(Me_2bipy)](ClO_4)) and laccase enzyme on non-functionalized and functionalized hexagonal mesoporous silica (HMS) supports or by direct synthesis of a Cu-substituted HMS mesoporous silica.

The materials were characterized by means of elemental analysis, FAA spectroscopy, small-angle powder XRD, nitrogen adsorption–desorption, SEM electron microscopy, TG-DTA analysis, and IR and UV–Vis spectroscopy. All the synthesized materials were tested for their catalytic activity on the oxidation of 4-aminoantipyridine, 2,2′-azinobis (3-ethyl-benzothiazoline)-sulfonic acid (ABTS) with air, and also in the liquid phase oxidation of anisole and phenol with hydrogen peroxide. The biomimetic behavior of the immobilized copper complexes was evidenced by comparing their oxidative catalytic activity with those of the laccase immobilized in the same supports.

Experimental

Synthesis of catalysts

Preparation of functionalized HMS silica

HMS mesoporous silica was synthesized using dodecylamine ($CH_3(CH_2)_{11}NH_2$) (Aldrich) as a template and tetraethoxysilane (TEOS, 98%, Aldrich) as silica precursor. For the HMS silica synthesis, a fixed ratio DDA: TEOS: H_2O: EtOH of 1:4:200:50 was used knowing that this ratio is important for the control of the morphology and pore structure [30, 31]. Dodecylamine was dissolved in a mixture of ethanol and H_2O and stirred for 30 min. TEOS was thereafter added drop wise under vigorous stirring. The mixture was stirred for 20 h at room temperature. The resulting precipitate was filtered and dried in air. The surfactant was removed by Soxhlet extraction with ethanol (24 h) then dried for 24 h at room temperature and 1 h at 373 K.

HMS was silanized with 3-aminopropyl-triethoxysilane (APTES) by a post-synthesis method according to a previously described procedure [32]. The NH_2-functionalized mesoporous silica (referred as NH_2-HMS) was filtered and washed with toluene, ethylic alcohol, and then diethyl ether. It was then submitted to a continuous extraction run overnight in a Soxhlet apparatus using diethyl ether/dichloromethane (v/v, 1/1) at 373 K and dried overnight at 403 K.

Preparation of Cu (II) complexes and the corresponding catalysts

The synthesis of the mononuclear [Cu(AA)(BB)](ClO_4) species is based on the reaction of an aqueous solution containing 2 mmols of $Cu(ClO_4)_2$ to which are simultaneously added an ethanolic solution containing 2 mmols of neutral chelatic ligand (phen, bipy, Me_2bipy) and an aqueous solution containing 2 mmols of acetyl acetone previously deprotonated with LiOH (Fig. 1). Crystals of [Cu(acac)(phen)(H_2O)](ClO_4), [Cu(acac)(bipy)(H_2O)](ClO_4), and [Cu(acac)(Me_2bipy)](ClO_4) are obtained through slow evaporation of the solvent at room temperature (η = 80–85%).

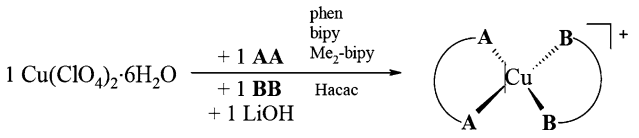

Fig. 1 The synthesis of monocationic $[Cu(AA)(BB)]^{+}$ complexes

0.1 g of copper complexes $[Cu(acac)(phen)(H_2O)]ClO_4$ (denoted C1) and $[Cu(acac)(Me_2bipy)]ClO_4$ (denoted C2) in 10 mL methanol was slowly added to 1 g of HMS or amine-functionalized HMS silica support in 20 mL methanol. The resultant mixture was refluxed for 24 h. The mixture was then filtered, washed with solvent, and dried under vacuum at room temperature. The copper content of the C1-NH_2-HMS and C2-NH_2-HMS samples was determined by FAA spectroscopy after their dissolution in 10% HF. The immobilization yield was calculated either from the TG/DTA analysis or as a difference between the complex concentrations of the initial and filtrate solutions, determined by UV–Vis spectrometry. The activity of Cu complexes immobilized on HMS silica was compared with that of Cu-substituted HMS. Cu-HMS was synthesized following a similar procedure with that proposed by Tanev et al. [26, 33, 34] via neutral templating pathway using dodecylamine as surfactant, copper chloride, and TEOS. The molar composition of the gel was: 5.24 SiO_2: 1 DDA: 0.13 $CuCl_2$: 345 H_2O: 47 EtOH. The solid precipitate was filtered, washed with ethanol, dried overnight at 393 K, and calcined at 873 K for 4 h. The copper content of the Cu-HMS samples was determined by FAA spectroscopy after their dissolution in 10% HF.

Immobilization of laccase into mesoporous silica supports

Laccase from *T. versicolor* (Sigma) with an activity of 34 U mg^{-1} protein was used without further purification. Immobilization of laccase was carried out by physical adsorption. In a typical procedure, 1 g support (HMS or NH_2-HMS) was mixed with 10 mL of 0.1 M phosphate buffer (pH 7.0) in a centrifuge tube. Thereafter, 50 mg laccase in 3 mL phosphate buffer were added to the mixture and homogenized under magnetic stirring at 278 K. In this suspension acetone (30 mL) was added drop wise and the stirring was continued for another 30 min. The solid was separated by centrifugation and washed several times with phosphate buffer until no laccase activity was detected in the washing. The immobilized systems were dried under vacuum and stored at 253 K, in dark. The amount of the enzyme immobilized on the support was calculated by the difference between amount of protein initially added and that recovered in the supernatants and washing buffer. Protein concentration in the supernatant was determined by Bradford procedure [35] using bovine serum albumin as standard.

Characterization

Adequate physico-chemical techniques were used to evaluate the solid structure, textural properties, and presence of the organic groups grafted on the silica surface. Small-angle X-ray powder diffraction (XRD) data were acquired on a Brucker diffractometer using CuKα radiation. N_2 adsorption–desorption isotherms were measured at 77 K with a Micromeritics ASAP 2010 instrument. FT-IR spectra of self-supported wafers previously heated at 423 K under vacuum were performed on a Bruker Vector 22 spectrometer. FT-IR spectra have been normalized with respect to the overtones of the silica bands at 1861 and 1960 cm^{-1}. Atomic adsorption spectroscopy (FAAS) measurements were performed on a Spectra AA-220 Varian spectrometer equipped with Varian multi-element hollow cathode lamps and air–acetylene burner. Thermogravimetric analysis was carried out in a Netzsch TG 209C thermobalance. About 15 mg of solid sample was loaded, and the air flow used was 50 cm^3 min^{-1}. The heating rate was 20 K min^{-1} and the final temperature was 1123 K. The organic phase content was obtained by CHN analysis using a CHN Perkin-Elmer analyzer, model 2400. The analysis was made after heating the materials at 373 K under vacuum for 1 h. The structures of Cu(II) complexes were determined using X-ray diffraction. The UV–Vis spectra of the synthesized copper complexes were recorded using a Thermo Scientific (Evolution 600) spectrometer.

Catalytic activity measurements

The catalysts obtained by immobilization of Cu(II) complexes, incorporation of Cu in HMS network, and immobilization of laccase were tested for their catalytic activity on the ABTS oxidation with air and on liquid phase oxidation of anisole and phenol with hydrogen peroxide. The activities of free and immobilized laccase were spectrophotometrically determined by the oxidation rate of 1 mM ABTS in 0.1 M acetate buffer (pH 4.5) at 296 K. The substrate solution was aerated by air bubbling before the addition of 10 μL of 5 mg L^{-1} enzyme solution for 3 mL reaction mixture. During the process, the increase in absorbance at 424 nm was measured ($\varepsilon = 36{,}000$ L mol^{-1} cm^{-1} for the oxidation product of ABTS). One unit of laccase activity was defined as the amount of enzyme required to oxidize 1 μmol ABTS per minute.

For the determination of immobilized laccase activity, 10 mg of active solids were added to 50 mL of 1 mM ABTS in 0.1 M acetate buffer (pH 4.5), which was allowed to circulate through the spectrophotometric cell thermostated at 296 K. The enzymatic activity was expressed in U/mg of immobilized protein or as relative activity:

$$\mathrm{EA}\% = \frac{U^{\mathrm{solid}}/\mathrm{mg}}{U^{\mathrm{solution}}/\mathrm{mg}} \times 100$$

The ABTS oxidation reaction in the presence of host-free complexes was monitorized in the same maner as for the free laccase. Still, in this case 300 mL of 100 mg L^{-1} complex solution in methanol was added to 3 mL reaction mixture. For the immobilized complexes, 50 mL of 1 mM ABTS in 0.1 M acetate buffer (pH 4.5) was used and the amounts of active solids were calculated in order to maintain the same amount of Cu(II) as in alcoholic solution of complexes. During the catalytic reaction, the absorbance was measured for 60 min and the initial rate of ABTS oxidation was obtained from the plots of ABTS oxidation product concentrations versus time. In order to make initial rates and conversions comparable, the reaction mixture always contained the same amount of Cu (II). The same procedure was applied for the Cu-HMS sample.

Oxidation of anisole and phenol with H_2O_2 was carried out at 303 K in a quartz mini reactor (5 mL). The reaction products were analyzed by gas chromatography and mass spectrometry.

Results and discussions

Properties of the catalyst precursors

Precursors of the catalysts are HMS support, functionalized NH_2-HMS support, and Cu(II) complexes. X-ray diffraction is a very effective technique for characterization of ordered mesoporous materials. As shown in Fig. 2, the modified samples show XRD patterns similar to that of the parent HMS, exhibiting a single reflection peak at 2.5° of 2θ, corresponding to lattice spacing of 4.9 nm. No significant changes upon amine immobilization were observed, except for the expected decrease in XRD peak intensity, providing the evidence that functionalization occurred mainly inside the mesopore channels. The diffraction peak at $2\theta = 2.5°$ may be due to the d_{100} reflection in materials with a short-range hexagonal order. Similar patterns have been reported for ordered mesoporous materials such as HMS [33]. As already noted, these HMS materials do not display the degree of long-range order associated with the MCM-41 class of silicates.

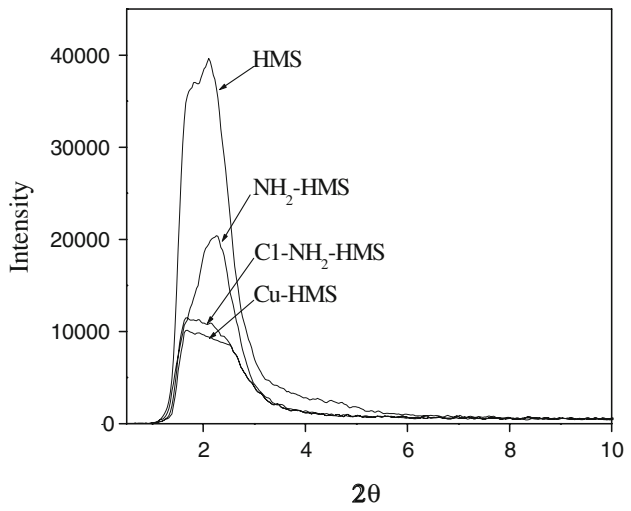

Fig. 2 Powder X-ray diffraction patterns of pure and modified HMS silica

The morphology of these materials, illustrated by SEM images, is characteristic for mesostructured silica materials. SEM images (Fig. 3a, b) of all the samples show small globular particles of around 1 μm in diameter.

The nitrogen adsorption isotherm at 77 K of the calcined HMS material (Fig. 4) is of type IV, featuring a sharp step corresponding to the filling of the ordered mesopores in the p/p_0 range of 0.1–0.5 and a H1 hysteresis loop at p/p_0 of 0.5 and therefore is typical of mesoporous materials. The surface area decreased for the NH_2-HMS sample (Table 1). For example, for the aminopropyl functionalized mesoporous silica (NH_2-HMS) the S_{BET} was diminished with 49.56%, comparatively to the HMS support. These textural results confirm that the grafted species are also located inside the mesopores and not only on the outer surface.

The amount and the density of the functional groups grafted on the HMS surface were determined by elemental and thermogravimetric analysis. Thus, the amount of grafted aminopropyl groups on HMS silica was 2.29 mmol/g (4.2 molecules/nm^2). The average number of silanol groups (quantified by ^{29}Si NMR spectroscopy) for the mesoporous silica is around 4 OH nm^{-2}. Based on this density of silanol groups, the calculated yield of the aminopropyl grafting was more than 100%. From the elemental analysis data it was also established that the C/N and H/N atom ratios in the NH_2-HMS sample were 6.7 and 17.86, respectively. This result suggests that the stoichiometry between the silanol group and the silylating agent was 1:1, indicating that most of aminopropyl silane chains are linked to the pore wall surface only by one Si–O–Si bond. The amount of aminopropyl groups grafted on the functionalized amorphous silica was 1.78 mmol g^{-1} SiO_2 (2.02 molecules nm^{-2}).

The infrared spectrum of the calcined HMS (Fig. 5) shows the typical Si–O lattice vibration: a strong and broad band with two peaks in the region 1450–900 cm^{-1} and two strong bands between 900 and 450 cm^{-1}. Furthermore, a very broad band present is centered at 3450 cm^{-1}, due to the O–H stretching vibrations. A band at 1618 cm^{-1} is also observed in the spectrum and is attributed to the H–O–H bending vibration of physisorbed water. Upon amine functionalization, a decrease in the intensity of the bands at 3450 and at 800 cm^{-1} is observed. Furthermore, the band

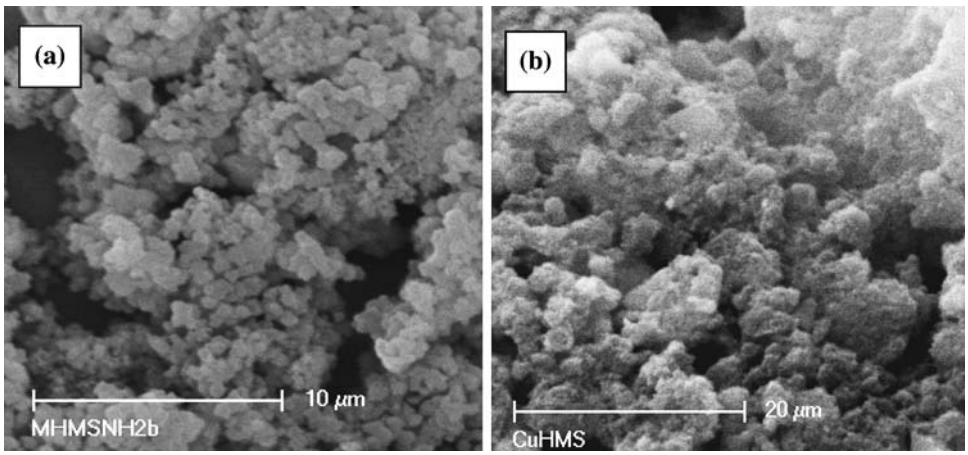

Fig. 3 SEM images of **a** NH_2-HMS silica and **b** Cu-HMS

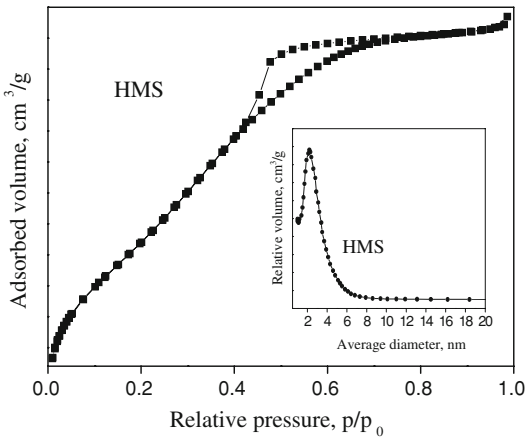

Fig. 4 N_2 adsorption–desorption isotherms of the HMS support and the corresponding pore size distribution (inset)

at 960 cm^{-1} disappeared indicating that the reaction between the isolated silanol groups of the HMS surface with the ethoxy groups of the silane derivative took place. The N–H and C–H stretching vibrations of APTES are observed in the region 3400–3000 cm^{-1} and 3000 cm^{-1}, respectively, and the corresponding H–N–H and H–C–H bending vibrations can also be observed in the region 1700–1500 cm^{-1} and 1500–1300 cm^{-1}.

The $[Cu(AA)(BB)](ClO_4)$ (AA = 1,10-phenantroline; 2,2′-bispyridyl; 4,4′-dimethyl-2,2′-bispyridyl; BB = acetylacetonate anion) complexes have been successfully used in the synthesis of some homo- and heteropolymetallic systems exhibiting interesting optical or magnetic properties, due to the existence of two potentially vacant coordination sites (ClO_4^- is weakly coordinated), the presence of chelating ligands containing delocalized π electrons, which can generate supramolecular architectures through π–π interactions, and the localization of the magnetic orbital in the basal plane that prevents the magnetic interactions mediated by the bridging ligands placed in the apical position. Crystals of $[Cu(acac)(phen)(H_2O)](ClO_4)$, $[Cu(acac)(bipy)(H_2O)](ClO_4)$, and $[Cu(acac)(Me_2bipy)](ClO_4)$ are obtained through slow evaporation of the solvent at room temperature (η = 80–85%). Their structures were determined using X-ray diffraction. $[Cu(acac)(phen)(H_2O)](ClO_4)$ and [Cu (acac) (bipy) (H_2O)] (ClO_4) have similar structures, with pentacoordinated Cu (II) ions, containing the acetylacetonate ligand, a 1,10-phenantroline or 2,2′-bispyridyl ligand in the basal plane of the pyramid, and a water molecule coordinated in the apical position (Fig. 6). The $[Cu(acac)(Me_2bipy)](ClO_4)$ complex contains a square-planar Cu(II) ion, the two chelatic ligands—acetylacetonate and Me_2bipy—being almost coplanar. The perchlorate anions are not coordinated (Fig. 7). The different stereochemistry of the Cu(II) ions in

Table 1 Textural properties of calcined HMS and modified HMS samples and the amounts of immobilized complexes in different supports

Sample	S_{BET} (m^2 g^{-1})	V_{meso} (ml g^{-1})	D (nm)	Cu content (μmol/g)	Spectro-photometric method (mg/g solid)	TG/DTA (mg/g solid)	Immobilization yield (%)
HMS	1029	0.79	3.5	–	–	–	–
C1-HMS	957	0.75	3.4	2	0.91	0.86	0.87
C2-HMS	985	0.77	3.5	1.6	0.72	0.69	0.68
NH_2-HMS	510	0.30	2.3	–	–	–	–
C1-NH_2-HMS	236	0.18	1.7	168	77.9	70.95	74.43
C2-NH_2-HMS	258	0.23	1.9	152	68.5	60.45	64.48

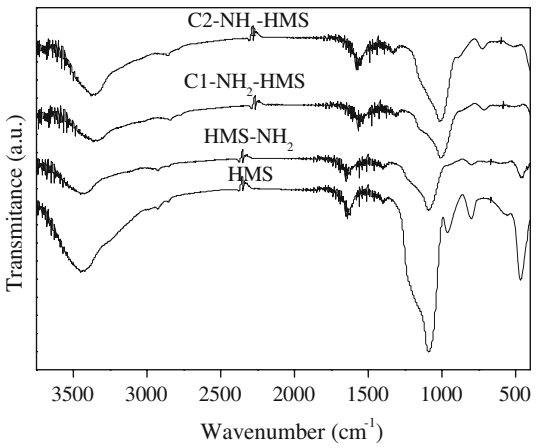

Fig. 5 FTIR spectra for unmodified HMS and functionalized HMS silica

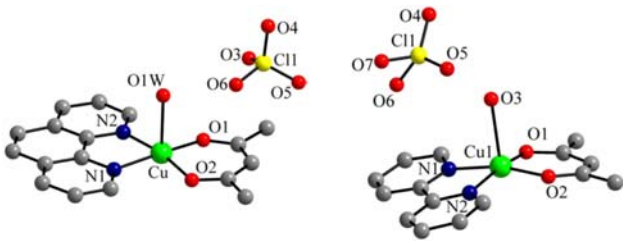

Fig. 6 The crystal structures of $[Cu(acac)(phen)(H_2O)](ClO_4)$ and $[Cu(acac)(bipy)(H_2O)](ClO_4)$

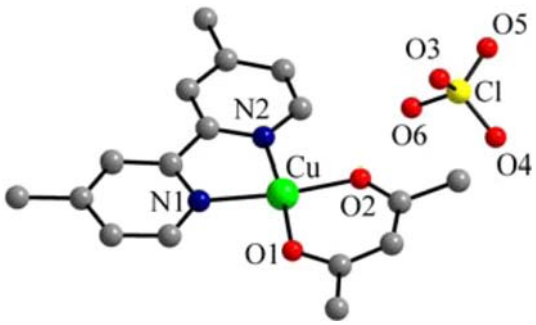

Fig. 7 The molecular unit of $[Cu(acac)(Me_2bipy)](ClO_4)$

the $[Cu(AA)(BB)](ClO_4)$ complexes was evidenced in the UV–Vis spectra by the differences in bands associated to the d–d transitions. $[Cu(acac)(phen)(H_2O)](ClO_4)$ and [Cu (acac)(bipy)$(H_2O)](ClO_4)$ complexes, having a CuN_2O_3 chromophoric group, give rise to blue crystals, while $[Cu(acac)(Me_2bipy)](ClO_4)$ is red-brown due to a CuN_2O_2 cromophore (Fig. 8). The intense absorption bands in the UV region (280–330 nm) can be related to the ligands which contain extended π electron systems: π(acac)–π(acac)*, π(phen)–π(phen)*, π(bipy)–π(bipy)*, and $\pi(Me_2bipy)$–$\pi(Me_2bipy)$* transitions. The absorption bands in the 405–415 nm region could be related to the charge transfer between the ligands and the metallic ions.

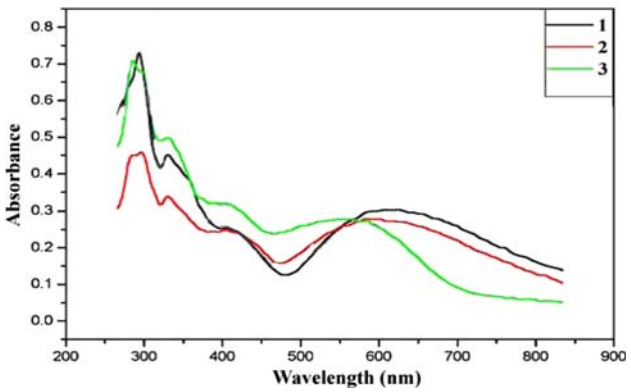

Fig. 8 Electronic spectra for the $[Cu(AA)(BB)](ClO_4)$ complexes: 1 = $[Cu(acac)(phen)(H_2O)](ClO_4)$; 2 = $[Cu(acac)(bipy)(H_2O)](ClO_4)$; 3 = $[Cu(acac)(Me_2bipy)](ClO_4)$

Physico-chemical properties of the catalysts

XRD pattern (Fig. 2) of Cu-HMS shows a peak at $2\theta < 3°$ corresponding to the [100] diffraction, indicating that this material posses a mesoporous local order without a long-range order. The d-spacing of the diffraction pattern for Cu-HMS increases slightly comparing with the corresponding one of HMS (from 4.9 to 5.3 nm). This behavior can be attributed to the copper incorporation into HMS network. Furthermore, the intensity of the reflection peak [100] slightly decreases due to a partial collapse of the HMS framework. According to FAA spectroscopy measurements after samples dissolution in HF, the amount of copper contained in the samples was 1.656 wt%, which was consistent with that of copper added into reaction mixture. The as-obtained copper substituted mesoporous silica could be an efficient catalyst for oxidation reactions, as well as a support for a biomimetic catalyst. The possible interactions between the stabilized cuprous species in the silica framework and the substrate could account for a significant enhancement of the catalytic performances.

Two copper (II) complexes with mixed ligands have been synthesized and subsequently immobilized on a HMS or amino-modified HMS silica supports from an alcoholic solution. The efficiency of the complexes immobilization was determined by a spectrophotometric method, by atomic absorption spectrometry and TG/DTA analysis. The obtained results are presented in Table 1. For the free HMS solids, the immobilization yields have very low values (under 1%). These values suggest that the two tested complexes were not practically immobilized. Contrarily, the amino-functionalized solids have proved to be more effective in complexes immobilization. The amount of copper from the solids containing immobilized complexes was determined by FAAS. The copper contents were 168 μmol/g for C1-NH_2-HMS material and 152 μmol/g for

C2-NH_2-HMS material, respectively. Relatively to the copper (II) complex amounts initially present in each alcoholic solution, the immobilization yields were 74.43% for C1, and 64.48% for C2, respectively. Considering the BET surface area (Table 1) of the amino-functionalized silica and the molecular surfaces of the immobilized complexes, the maximum estimated capacity of complex immobilization was around 550 μmol/g. Furthermore, the amino groups on the HMS surface are always in great excess relative to the complex. The difference between the theoretical and practical complex content in functionalized HMS materials is due to the diffusion control of the metal complex immobilization reaction. These values of the copper amounts are in agreement with the copper contents calculated from the amount of immobilized complex (determined by UV–Vis measurements). These results suggest that the immobilized copper (II) species have the same structure throughout the HMS matrix as in the alcoholic solution.

The thermal decomposition of the C1 and C2 complexes and of the host–guest materials (C1-NH_2-HMS and C2-NH_2-HMS) were also studied by thermogravimetry (TG) and differential thermal analysis (DTG). The thermal decomposition curves of the supported complexes (not shown) indicate that the immobilization was successful on modified mesoporous silica. Namely, dehydration could always be observed between 373 and 473 K. The thermal decomposition of the organic ligand occurred between 523 and 823 K for the C1-NH_2-HMS sample, and between 523 and 723 K, for the C2-NH_2-HMS sample, respectively. For the free complexes (C1 and C2) the organic ligand decomposition occurred between 473 and 1023 K.

Upon complex immobilization in the functionalized silica framework, a diminution of the intensity of the main diffraction peak and a slightly decrease in the *d* spacing value (3.5 nm) were observed in the XRD patterns (Fig. 2), confirming that the short-range hexagonal order was preserved.

No change in the isotherm profile was observed upon complex immobilization, suggesting that the functionalized HMS structure was unaffected by complex anchoring. However, a further decrease in the material surface area and a slight decrease in the mean mesopores size are observed, confirming indirectly the presence of the complex within the matrices.

The IR spectra of C1-NH_2-HMS and C2-NH_2-HMS show some changes with respect to the parent material in regions where vibration from APTES occur: 3500–3000 cm^{-1} region, due to N–H stretching vibrations and 1700–1300 cm^{-1}, with absorptions due to the H–N–H and H–C–H bending vibrations, suggesting some molecular changes in the spacer. On the other hand, broad bands are observed at about 1658 and 1555 cm^{-1}, which may be attributed to a C=N stretching vibration and to the metal complex acetylacetonate ring vibrations, respectively. C–H stretching vibrations (from phen or dipy rings) appear above 3000 cm^{-1} and characteristic C–H out of plane bending vibrations are seen at about 879 and 729 cm^{-1}, indicating the presence of diimine ligands. These results indicate that there was a Schiff condensation between the free amine groups on the surface of the HMS material and the oxygen atoms coordinated to copper (II), and therefore the complex anchoring occurred as depicted in Scheme 1.

Laccases (*p*-diphenol: dioxygen oxidoreductase, E.C. 1.10.3.2) are multi-copper oxidase having Types 1, 2, and 3 copper sites [36]. Laccases reduce oxygen directly to water in four-electron transfer step without intermediate formation of soluble hydrogen peroxide in expense of one-electron oxidation of a variety of substrates, e.g., phenolic compounds [37].

Trametes versicolor laccase is a globular proteine having $5 \times 5 \times 7$ nm^3 dimensions and a molecular weight of 60 kDa. These dimensions allow the enzyme accommodation into micro- and mesopores with diameters higher than 10 nm. As a general rule, the pore dimensions must be the same order of magnitude as the maximum protein dimensions in order to allow an efficient retention and the free passing of the substrates and reaction products. *Trametes versicolor* laccase was immobilized by adsorption into HMS or amino-functionalized HMS mesoporous silica in order to obtain an efficient catalyst for the ABTS substrate oxidation. The oxidative catalytic activities of these ones were compared with those of the immobilized copper complexes or of the copper substituted HMS silica. The same support was used in all the immobilization procedures.

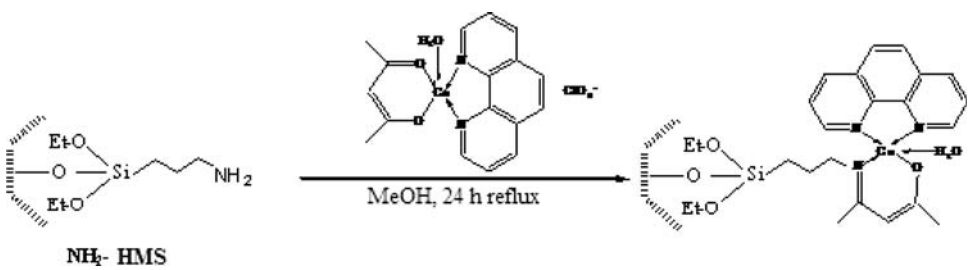

Scheme 1 Suggested model for the anchoring of $[Cu(acac)(phen)(H_2O)]ClO_4$ complex onto NH_2-HMS

Table 2 The amount and enzymatic activity of immobilized laccase in HMS supports

Sample	Bradford method (mg/g solid)	TG/DTA (mg/g solid)	Immobilization yield (%)	Enzymatic activity (UI/mg proteine)	Relative enzymatic activity (%)
L-HMS	30.36	28.50	40.93	16.73	50.68
L-NH_2-HMS	133.03	128.94	81.86	23.27	70.45

The amount of immobilized enzyme was determined either as equivalent bovine serum albumin (BSA) protein determined by Bradford method or as organic mass loss from TG-DTG curves (Table 2).

In the case of HMS-type silica, the enzyme immobilization yields are lower than other mesoporous silica materials (SBA-15, MCM-41) due to the irregular pore size distribution and the diffusion limitations. The higher yield obtained for the laccase immobilization into the amino-functionalized HMS silica is probably due to the stronger interactions between the enzyme functional groups (–NH_2, –COOH, –OH, –SH) and that of the support surface. For enzyme immobilization the acetone was added to a mixture of the solid support and the buffered enzyme solution in order to produce a forced diffusion of the enzyme into the hydrofile pores. This method is more efficient than other adsorption methods when much more parameters (such as pH, contact time, temperature, etc.) must be considered.

The immobilization yields (Table 2) obtained with this method are consistent with the results of other research studies on the same type of supports reported in the literature.

Catalytic properties of the catalysts

Catalytic activities of the host-free and immobilized complexes, as well as Cu modified HMS silica was tested in two steps. The preliminary tests were performed by oxidation with air of ABTS. The results were evaluated from the absorption band of ABTS oxidation product at 424 nm using a Cu(II): ABTS ratio of 1:42. The pH value was kept at 4.5 with acetate buffer and the solution was saturated in oxygen by air bubbling before the starting of the catalytic test. ABTS oxidation measurements revealed the catalytic activities of the complexes—free or immobilized—and copper substituted silica. The initial rate values (calculated from the concentration of ABTS oxidation product versus time graph) are given in Fig. 9. The calculated initial rate values of the host-free complexes (C1 and C2) are about the same (0.48 and 0.50 μM min^{-1}, respectively). The activity of the C1 and C2 complexes significantly changed upon immobilization (18.85 and 28.81 μM min^{-1}, respectively). The most active material toward ABTS oxidation was the [Cu(acac)(Me_2bipy)]ClO_4 (C2) complex immobilized into amino-functionalized HMS mesoporous silica,

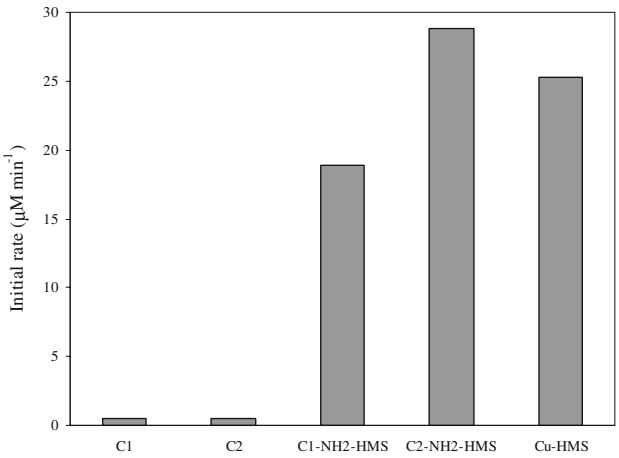

Fig. 9 The initial rate values of host-free and immobilized copper (II) complexes and Cu-HMS in the ABTS oxidation reaction

having nearly 58-fold higher activity than in the case of the host-free complex. The initial rate of the ABTS oxidation was higher for both copper complexes after immobilization than for the host-free complexes. This is probably due to additional interactions of the substrate with the support matrix. The catalytic activity of copper-substituted HMS silica (25.23 μM min^{-1}) is close to the C2 immobilized complex.

In order to evaluate the efficiency of the immobilized copper complexes and of the copper-substituted HMS silica, laccase from *T. versicolor* immobilized in the same solid supports was tested also in the ABTS oxidation reaction. The activity of free laccase toward ABTS oxidation with air was firstly determined (33.3 U mg^{-1}).

The enzymatic activity and the relative activity of the immobilized laccase are given in Table 2. The obtained values suggest that the immobilized laccase posses a much higher oxidative catalytic activity (about 10^3 times) than the biomimetic catalysts. Furthermore, the laccase activity strongly depends on the support surface nature. Thus, the amino-functionalized silica allows the immobilization of a greater amount of protein, and consequently the enzymatic activity is higher.

Unlike complexes, a decrease of the enzymatic activity was evidenced upon enzyme immobilization. This behavior can be attributed to the more difficult diffusion of the

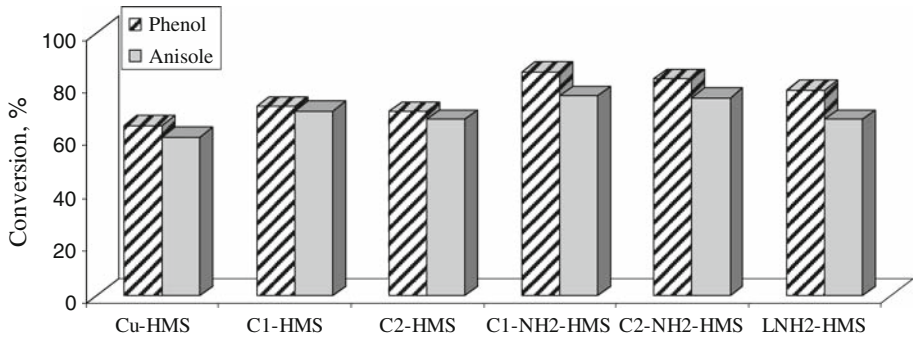

Fig. 10 Catalytic activity in oxidation of aromatic hydrocarbons with hydrogen peroxide

substrate to the active sites of the enzymes due to their tertiary structure.

The activity of the samples in oxidation of aromatic compounds such as anisole and phenol was very high (Fig. 10). It can be shown that Cu (II) complexes are more active than supported laccase and Cu-HMS catalysts.

Phenol and 2-methoxyphenol were identified between reaction products in the case of anisole oxidation, and acid acetic, *p*-benzoquinone and 1,2-benzene diol for phenol oxidation. The higher selectivity was evidenced for hydroxylation at benzene ring with the formation of 2-methoxyphenol or 1,2-benzene diol. For phenol, the main product was 1,2-benzene diol. Nevertheless, the oxidative degradation of the substrate occurred in all the reaction, especially in oxidation performed on immobilized laccase. In this case, only oxidative degradation was evidenced for phenol, while for anisole, *o*-methoxyphenol, phenol, and 4-methoxyphenol were identified in the reaction products.

Conclusions

New biomimetic catalysts were obtained by immobilization of $[Cu(AcAc)(Phen)(H_2O)]ClO_4$, $[Cu(AcAc)(Me_2bipy)]ClO_4$ complexes on HMS or NH_2-functionalized mesoporous silica. The copper-substituted HMS silica with a mesoporous structure was synthesized using neutral templating pathway at the room temperature. In order to verify the complexes biomimetic activity, the *Trametes versicolor* laccase was immobilized by adsorption in the same supports. The successful anchoring of the metal complexes over the supports and the structural integrity of the mesoporous hosts were confirmed by various characterization techniques. The organic functional groups, the tested biomimetic complexes, and the enzyme were successfully grafted on the HMS surfaces and the ordering of the support was not affected by the immobilization. The structure of the mesoporous materials was not affected by the cooper substitution in the silica framework. The catalytic tests showed catalytic activity toward ABTS oxidation reaction and oxidation of aromatic compounds (anisole, phenol) for all the investigated catalysts. The oxidation activities of complexes after immobilization have been proved to be higher than in homogeneous phase.

The copper-substituted mesoporous silica could be a good catalyst for oxidation of aromatic compounds or a very good support for biomimetic oxidation catalyst due to the possible interactions between the metallic ions of the biomimetic complex and the stabilized cuprous species in the silica framework.

Acknowledgements Financial support from the Romanian Education and Research Ministry in the Framework of CeEx project no. 50/2006 is gratefully acknowledged.

References

1. Dıaz U, Cantın A, Corma A (2007) Chem Mater 19:3686
2. Parvulescu AN, Marin G, Suwinska K, Kravtsov VCh, Andruh M, Parvulescu V, Parvulescu VI (2005) J Mater Chem 15:4234
3. Roesky HW, Andruh M (2003) Coord Chem Rev 236:91
4. Wegner R, Gottschaldt M, Gorls H, Jager E-G, Klemm D (2001) Chem Eur J 7:2143
5. Kaizer J, Papp J, Speier G, Parkanyi L, Korecz L, Rockenbauer A (2002) J Inorg Biochem 91:190
6. Mimmi MC, Gullotti M, Santagostini L, Saladino A, Casella L, Monzani E, Pagliarin R (2003) J Mol Catal A Chem 204–205:381
7. Anisia KS, Kumar A (2007) J Mol Catal A Chem 271:164
8. Maurya MR, Chandrakar AK, Chand S (2007) J Mol Catal A Chem 270:225
9. Bao F, Ma R, Jiao Y (2007) J Coord Chem 60:557
10. Gao Y, Liu J, Wang M, Na Y, Akermark B, Sun L (2007) Tetrahedron 63:1987
11. Zois D, Vartzouma C, Deligiannakis Y, Hadjiliadis N, Monzani L, Louloudi M (2007) J Mol Catal A Chem 261:306
12. Szilagyi I, Horvath L, Labadi I, Hernadi K, Palinko I, Kiss T (2006) Cent Eur J Chem 4:118
13. Zois D, Vartzouma C, Deligiannakis Y, Hadjiliadis N, Casella L, Monzani E, Louloudi M (2007) J Mol Catal A Chem 261:306
14. Xia Q-H, Ge H-Q, Ze C-P, Liu Z-M, Su K-X (2005) Chem Rev 105:1603
15. Li C (2004) Catal Rev 46:419
16. Fan Q-H, Li Y-M, Chan ASC (2002) Chem Rev 102:3385
17. Brunel D, Belloq N, Sutra P, Cauvel A, Laspéras M, Moreau P, Di Renzo F, Galarneau A, Fajula F (1998) Coord Chem Rev 1085:178
18. Leadbeater NE, Marco M (2002) Chem Rev 102:3217
19. Rafelt JS, Clark JH (2000) Catal Today 57:33

20. Lakshumi Kantam M, Kavita B, Neeraja V, Haritha Y, Chaudhuri MK, Dehury SK (2003) Tetrahedron Lett 44:9029
21. Silva AR, Figueiredo JL, Freire C, de Castro B (2005) Catal Today 102–103:154
22. Silva AR, Freire C, de Castro B, Freitas MMA, Figueiredo JL (2002) Langmuir 18:8017
23. Ferreira R, Silva M, Freire C, de Castro B, Figueiredo JL (2000) Microporous Mesoporous Mater 38:391
24. Murphy EF, Ferri D, Baiker A, Van Doorslaer S, Schweiger A (2003) Inorg Chem 42:2559
25. Hu X, Zhao X, Hwang H (2007) Chemosphere 66:1618
26. Louloudi M, Mitopoulou K, Evaggelou E, Deligiannakis Y, Hadjiliadis N (2003) J Mol Catal A Chem 198:231
27. Tanev PT, Pinnavaia TJ (1995) Science 267:865
28. Macquarrie DJ, Jackson DB, Mdoe JEG (1999) New J Chem 23:539
29. Zhang W, Pauly TR, Pinnavaia TJ (1997) Chem Mater 9:2491
30. Lee H, Zi J (2001) Sep Sci Technol 36:2429
31. Di Renzo F, Testa F, Chen JD, Cambon H, Galarneau A, Plee D, Fajula F (1999) Microporous Mesoporous Mater 28:437
32. Brunel D, Cauvel A, Fajula F, Di Renzo F (1995) Stud Surf Sci Catal 97:173
33. Pauly TR, Pinnavaia TJ (2001) Chem Mater 13:987
34. Zhang P, Zhang Z, Wang S, Ma X (2007) Catal Commun 8:21. 44
35. Bradford MM (1976) Anal Biochem 72:248
36. Kim Y, Cho NS, Eom TJ, Shin W (2007) Bull Korean Chem Soc 23:985
37. Timur S, Pazarlioglu N, Pilloton R, Telefoncu A (2004) Sens Actuators B 97:132